THE ASTRONOMICAL JOURNAL, 118:261–272, 1999 July

OBSERVATION OF THE HALO OF THE EDGE-ON GALAXY IC 5249

F. ABE,[1] I. A. BOND,[2,3] B. S. CARTER,[4] R. J. DODD,[4] M. FUJIMOTO,[5] J. B. HEARNSHAW,[3] M. HONDA,[6] J. JUGAKU,[7] S. KABE,[8] P. M. KILMARTIN,[2,3] B. S. KORIBALSKI,[9] M. KOBAYASHI,[8] K. MASUDA,[1] Y. MATSUBARA,[1] M. MIYAMOTO,[10] Y. MURAKI,[1] T. NAKAMURA,[11] G. R. NANKIVELL,[4] S. NODA,[1] G. S. PENNYCOOK,[2] L. Z. PIPE,[2] N. J. RATTENBURY,[2] M. REID,[12] N. J. RUMSEY,[4] TO. SAITO,[13] H. SATO,[11] S. SATO,[5] M. SEKIGUCHI,[6] D. J. SULLIVAN,[12] T. SUMI,[1] Y. WATASE,[8] T. YANAGISAWA,[1] P. C. M. YOCK,[2] AND M. YOSHIZAWA[10]

(The MOA Collaboration)

Received 1998 May 21; accepted 1999 April 5

ABSTRACT

Optical photometry and H I synthesis observations of the southern edge-on Sc/Sd galaxy IC 5249 are reported. The rotation curve rises linearly out to a radius of 7 kpc and then appears to flatten out at ~ 100 km s^{-1}. The H I mass out to 24.5 kpc is $\sim 6 \times 10^9$ $M_\odot$, or 10% of the total mass out to this radius. The color, central surface brightness, scale height, and scale length of the disk of IC 5249 are $R - I \approx 0.4$, $\mu = 20.6 \pm 0.1$ R_C mag arcsec^{-2}, 600 ± 40 pc, and 11 ± 2 kpc, respectively. Additional light to that predicted by an exponential disk is present at distances greater than 3 kpc from the disk. At 5 kpc the surface brightness is 27–28 R_C mag arcsec^{-2}. The measured distribution of surface brightness is used to constrain the abundance of low-mass main-sequence stars in the halo of the galaxy. A halo made up entirely of main-sequence stars heavier than 0.13 $M_\odot$ is excluded. We also find that less than 20% of the halo can be composed of main-sequence stars heavier than 0.30 $M_\odot$. Further observations are required to determine the rotation curve of IC 5249 to large radii and to determine precisely the abundance of low-mass main-sequence stars in the halo of the galaxy.

Key words: dark matter — galaxies: halos — galaxies: individual (IC 5249) — galaxies: photometry — galaxies: structure — ISM: H I

1. INTRODUCTION

The composition of the dark matter in the Galactic halo remains unknown despite extensive efforts that have been made in recent years to identify it using a variety of techniques, including gravitational microlensing (Stubbs 1998) and the direct observation of low-mass stars (Flynn 1998; Tinney 1999).

A New Zealand–Japan collaboration called MOA has recently commenced a gravitational microlensing survey of the Magellanic Clouds and the Galactic bulge similar to those being undertaken by the MACHO, EROS, and OGLE groups (Abe et al. 1997; Alcock et al. 1997). The project is based at the Mount John University Observatory (MJUO) in New Zealand. In conjunction with the microlensing program, several exposures of the southern edge-on Sc/Sd disk galaxy IC 5249 were made to determine the abundance of low-mass main-sequence stars in the halo of this galaxy. The exposures were motivated in part by the previously raised possibility that the northern edge-on Sc galaxy NGC 5907 has a faint, visible halo surrounding its disk that traces its dark halo (Sackett et al. 1994; Fuchs 1995; Lequeux et al. 1996).

Results of our observations of IC 5249 are reported here, together with the results of H I synthesis observations of the galaxy that had been made previously using the Australia Telescope Compact Array (ATCA).

2. PREVIOUS OBSERVATIONS OF IC 5249

The galaxy IC 5249 was included in the Southern Sky Redshift Survey (da Costa et al. 1991) and in the Southern Sky Survey (Mathewson et al. 1992). Relevant parameters taken from the surveys are the type, Sc or Sd; inclination, $\approx 89°$; $m_I \approx 13.1$; central surface brightness $\mu_I \approx 20.1$ mag arcsec^{-2}; H I flux ≈ 27.85 Jy km s^{-1}; recession velocity (optical) ≈ 2332 km s^{-1}; recession velocity (H I) ≈ 2364 km s^{-1}; recession velocity (Tully-Fisher) $\approx 2320 \pm 100$ km s^{-1}; rotation velocity (H I) ≈ 102 km s^{-1}; major- and minor-axis diameters of $I_{23.5}$ isophote 184″ and 17″, respectively.

3. NEW H I MEASUREMENTS OF IC 5249

3.1. *ATCA* H I *Observations and Data Reduction*

H I synthesis observations of the galaxy IC 5249 were

[1] Solar-Terrestrial Environment Laboratory, Nagoya University, Furo-cho, Chikusa-ku, Nagoya 464-8601, Japan.
[2] Faculty of Science, University of Auckland, Private Bag 92019, Auckland, New Zealand.
[3] Department of Physics and Astronomy, University of Canterbury, Ernest Rutherford Building, Christchurch, New Zealand.
[4] Carter National Observatory, P.O. Box 2909, Wellington, New Zealand.
[5] Department of Physics, Nagoya University, Furo-cho, Chikusa-ku, Nagoya 464-8602, Japan.
[6] Institute for Cosmic Ray Research, University of Tokyo, 3-2-1 Midori-cho, Tanashi 188-8502, Japan.
[7] Research Institute of Civilization, 2-29-3 Sakuragaoka, Tama-shi 206-0013, Japan.
[8] High Energy Accelerator Research Organization (KEK), 1-1 Oho, Tsukuba 305-0801, Japan.
[9] Australia Telescope National Facility, CSIRO, P.O. Box 76, Epping, New South Wales 2121, Australia.
[10] National Astronomical Observatory, 2-21-1 Osawa, Mitaka 181-8588, Japan.
[11] Department of Physics, Kyoto University, Oiwake-cho, Kita-Shirakawa, Sakyo-ku, Kyoto 606-8224, Japan.
[12] Department of Physics, Victoria University of Wellington, P.O. Box 600, Wellington, New Zealand.
[13] Tokyo Metropolitan College of Aeronautics, 8-52-1 Minami-senjyu, Arakawa-ku, Tokyo 116-0003, Japan.

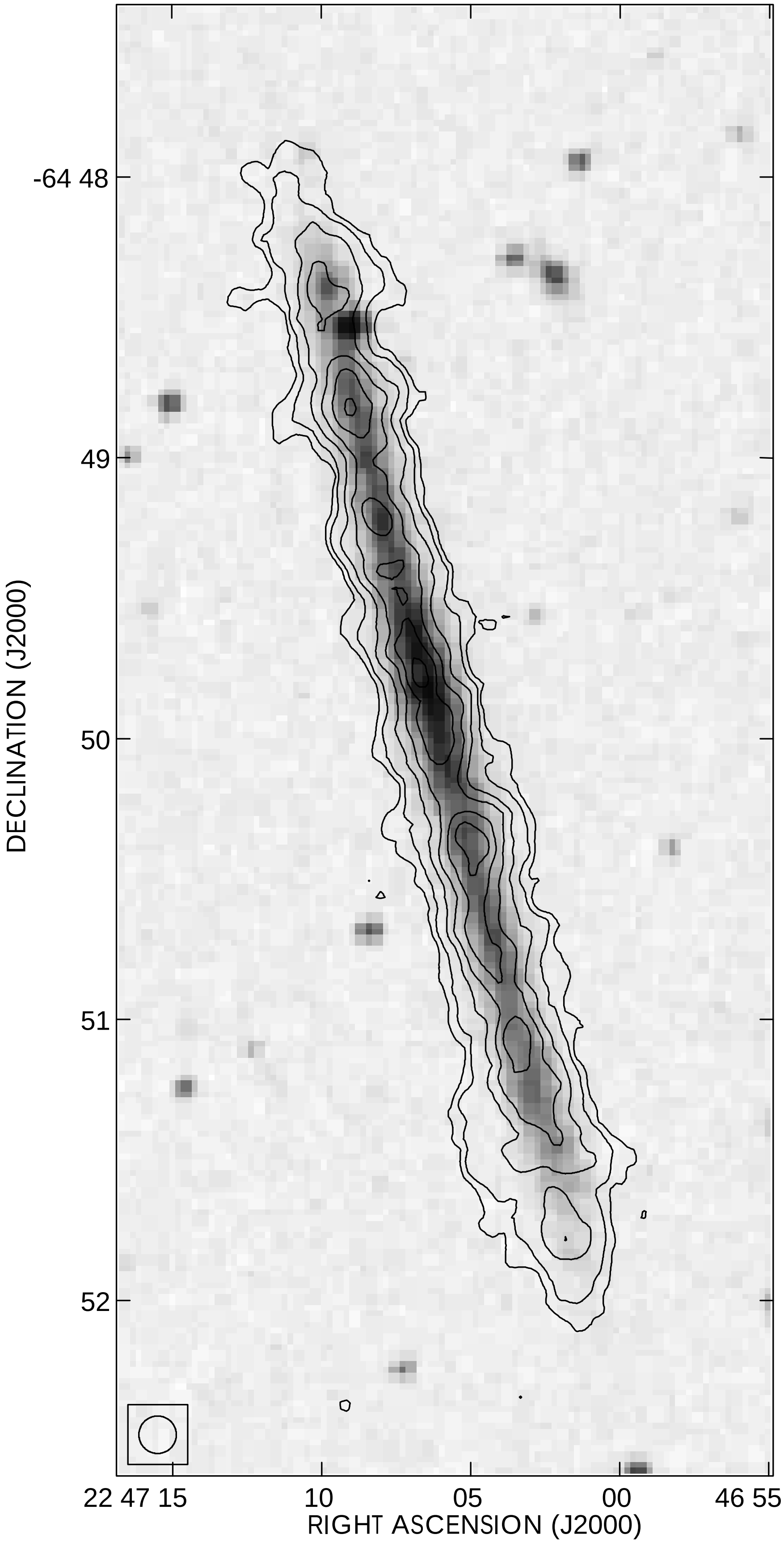

FIG. 1.—H I distribution of the galaxy IC 5249 overlaid on an optical image obtained from the Digital Sky Survey (DSS). The contour levels are 0.05, 0.1, 0.2, 0.3, 0.4, and 0.5 Jy beam^{-1} km s^{-1}, and the angular resolution is 8″. North is to the top, and east to the left. (The DSS was produced by the Space Telescope Science Institute and is based on photographic data from the UK Schmidt Telescope, the Royal Observatory Edinburgh, the UK Science and Engineering Research Council, and the Anglo-Australian Observatory.)

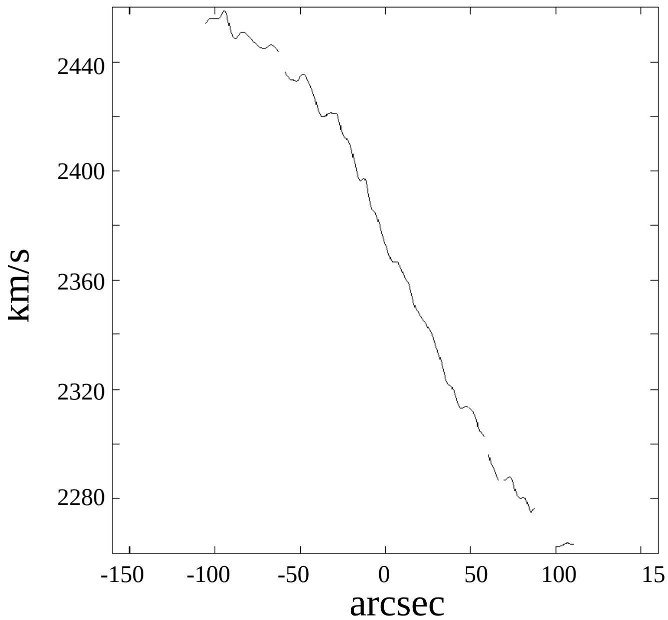

FIG. 2.—H I rotation curve of IC 5249. On the x-axis, negative offsets are roughly toward the south and positive offsets roughly toward the north.

obtained with the 6C configuration of ATCA[14] on 1992 October 18 by Levasseur, Carignan, & Byun (Levasseur et al. 1992). The total time on source was about 12 hours. The 8 MHz bandwidth centered on 1409 MHz was divided into 512 channels, which resulted in a velocity resolution of 3.35 km s^{-1}.

The data reduction and analysis was carried out with the AIPS software package using mostly standard procedures. The (u, v) data were inspected to find those channels containing H I emission. No 20 cm radio continuum emission was detected at the position of IC 5249 ($S_{\rm peak} < 1.5$ mJy $\rm beam^{-1}$). The brightest radio source we detected in the field is PMN J2248−6456 with a flux density of about 27 mJy (Wright et al. 1994). The H I line data were Fourier-transformed and then cleaned. Use of "robust weighting" (ROBUST = 1) resulted in an rms noise of ∼2.5 mJy $\rm beam^{-1}$ per channel and an angular resolution of 8″. IC 5249 was the only source detected in H I; neither of the galaxies at a projected distance of only 5′, AM 2243−650 and IC 5246, were detected in the given velocity range.[15]

3.2. *The Neutral Hydrogen Distribution and Kinematics*

Figure 1 shows the H I distribution (0.moment) overlaid onto an optical image of IC 5249. The H I extent of the galaxy is about 280″ × 24″ (at $N_{\rm H\,I} = 9 \times 10^{20}$ atoms $\rm cm^{-2}$) compared with 246″ × 22″ in the optical at R_{25} (see Fig. 7 below). The major-axis position angle is P.A. = 194°. We find an integrated H I flux of ∼20 Jy km s^{-1}, corresponding to an H I mass of about $6 \times 10^9\ M_\odot$ for IC 5249 assuming a distance of 36 Mpc. This is considerably lower than the total H I flux (27.85 Jy km s^{-1}) quoted by Mathewson et al. (1992) using the 64 m Parkes radio telescope and indicates that there is more extended hydrogen emission, which has been filtered out with the ATCA interferometer. The current H I distribution shows no evidence of flaring or warping, but more data are needed to study the faint extended structure beyond the optical R_{25} extent of IC 5249, where warps usually start (see, e.g., Briggs 1990).

The rotation curve of IC 5249, which was obtained by averaging the H I velocity field (1.moment) along a position angle at P.A. = 194° (width 22″), is displayed in Figure 2. The systemic velocity of the galaxy is ≈2365 km s^{-1}. We observe a linear rise of the rotation velocity within a radius of $r = 40''$.[16] Beyond that radius the rotation curve slowly turns over and seems to flatten at about $r = 100''$ or 17.5 kpc, although more sensitive data are needed to confirm this. The maximum observed rotational velocity is about 100 km s^{-1}. The total mass of IC 5249 within the observed H I disk (i.e., $r < 140''$ or 24.5 kpc) is about $5.7 \times 10^{10}\ M_\odot$. This assumes the mass inside 24.5 kpc is distributed approximately spherically and yields a mass ratio $\log (M_{\rm H\,I}/M_{\rm tot}) \approx -0.98$. This correlates well with the expected value of roughly −1 for Sc/Sd galaxies (Roberts & Haynes 1994).

4. PHOTOMETRIC MEASUREMENTS

IC 5249 was observed on the nights of 1997 July 4 and 6 with the 0.6 m Boller and Chivens telescope and one of the CCD cameras (MOA-cam1) that is used by the MOA collaboration. The telescope had previously been modified with the installation of wide-angle optics (1°.3 field) and a stepping motor drive system. MOA-cam1 has nine, unthinned 1K × 1K Texas Instrument type TC215 chips and has been described elsewhere (Abe et al. 1997). The chips are arranged in a 3 × 3 matrix, with spacing between adjacent chips equal to 0.9 times the width of a chip. The pixel size on the sky is 0″.645. The chip gain and readout noise are ≈8 e^- $\rm ADU^{-1}$ and 1.5 ADU, respectively.[17] A "step function" filter was used for the present measurements with ≈90% transmittance from 630 to 1000 nm. This includes ≈60% of the $R_{\rm C}$ passband and all the $I_{\rm C}$ passband. The cataloged quantum efficiencies of the Texas Instrument chip at these wavelengths are ∼55% and 40%, respectively. We confirmed, by direct measurement of a sample of chips, the catalog value in the $R_{\rm C}$ passband but found a somewhat lower efficiency ∼25% in the $I_{\rm C}$ passband (M. Honda 1999, private communication). The typical sky background at the observatory is $R_{\rm C} \approx 20.9$ and $I_{\rm C} \sim 19$ mag $\rm arcsec^{-2}$ and the typical FWHM seeing is 1″.5 to 3″.

The visible diameter of IC 5249 of 4′ enabled it to be accommodated on a single chip of MOA-cam1 with a large surrounding area of sky. Only three chips of the camera were used for the present observations, the top left (northeast) one, the center one, and the bottom right (southwest) one. Seven 20 minute exposures were made with the galaxy on the northeast chip, seven with the galaxy on the center chip, and seven with the galaxy on the southwest

[14] The Australia Telescope is funded by the Commonwealth of Australia for operation as a National Facility managed by CSIRO.

[15] IC 5246 is shown in Fig. 4 below. The recession velocities of AM 2243−650 and IC 5246 are unknown.

[16] In an edge-on galaxy, each rotation velocity measurement is an average of different contributions along the line of sight and therefore lower than if the major axis only could be observed. We assume most gas is concentrated in the main body of the galaxy and that this effect is small.

[17] ADU denotes analog-to-digital unit. The gain was confirmed in the present measurements using the known fluxes from standard stars (see § 5.2 below), and the read-out noise from the dark exposures (see § 5.1 below).

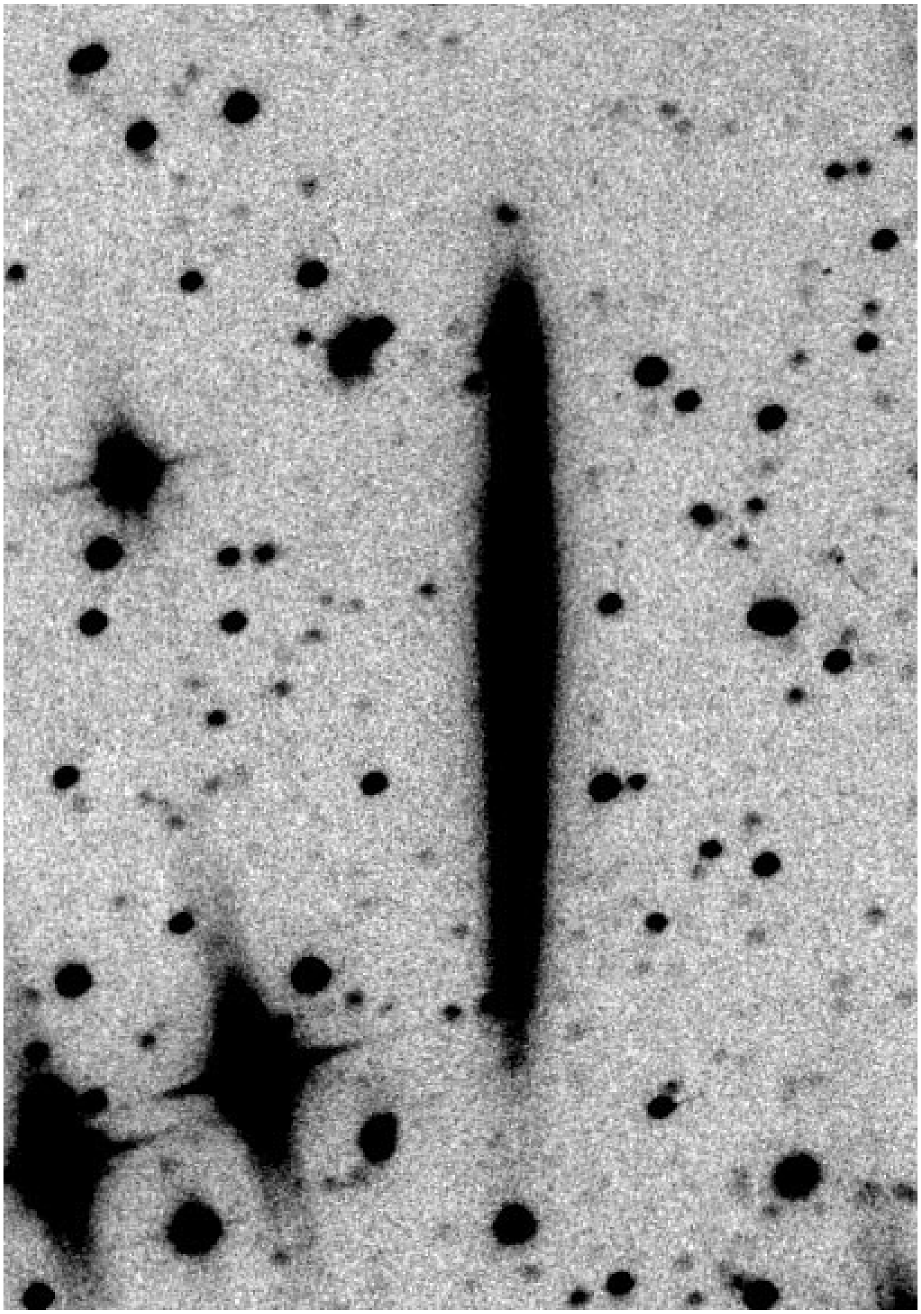

FIG. 3.—Stacked 5 1/3 hr image of IC 5249. The orientation is similar to that in Fig. 4 below, but with a 14° rotation applied to align the galaxy vertically. The gray scale is -3.5 ADU pixel^{-1} (white) to $+9.4$ ADU pixel^{-1} (black) per 20 minutes of exposure time.

chip[18]. Each of these exposures provided two exposures of sky on the two chips not being used for the galaxy. Another seven 20 minute dark exposures were also made on all the chips. Finally, numerous bias and short exposures were made. The exposures were carried out cyclically to minimize effects of changing air mass and changing camera temperature during a night. Offsets of the telescope of order 40″ or 70 pixels were made between repeat exposures of the same target (Pennycook 1998). Sky conditions on both the observing nights were photometric, and the seeing was approximately 3″.

5. REDUCTION OF PHOTOMETRY

5.1. *Frame Stacking*

A frame stacking technique similar to that of Morrison et al. (1994) was used to combine the images of IC 5249 (Pennycook 1998).

First, the 20 minute dark frames were compared with the bias frames. It was found that the dark current was negligible. Consequently, bias frames were subtracted from the galaxy and sky frames.

Flat fields were formed from the fourteen 20 minute sky

[18] A similar viewing procedure was employed by Lequeux et al. (1998). Exposures on different chips enable some causes of sky nonuniformities to be evaluated, as discussed in § 6.1 below.

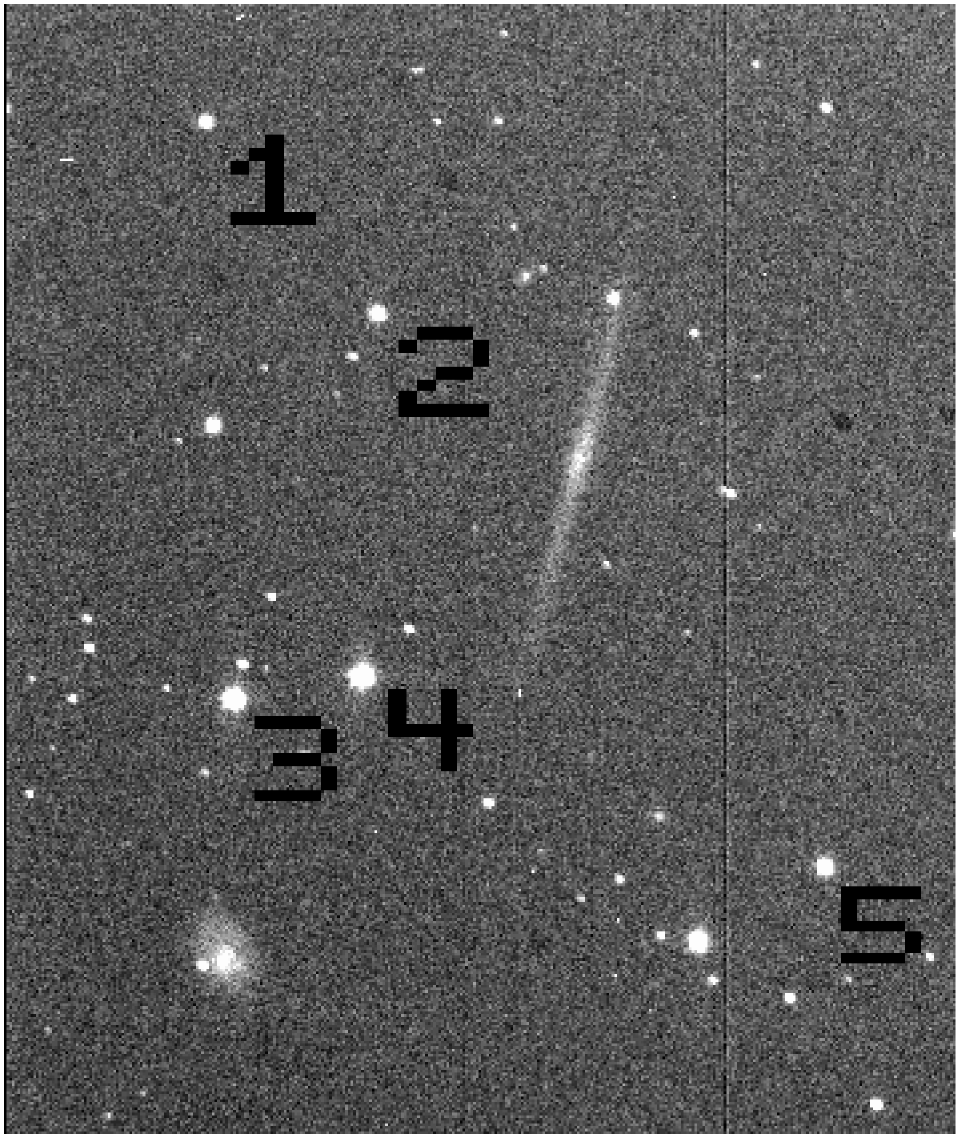

FIG. 4.—Five stars used to calibrate the photometry of IC 5249. North is to the top, and east is to the right. The V, B, R_C, and I_C magnitudes of stars 1, 2, 3, 4, and 5 are (14.41, 15.22, 13.91, 13.74), (14.03, 14.94, 13.53, 13.09), (12.33, 13.12, 11.90, 11.54), (12.08, 12.94, 11.67, . . .), and (13.29, 15.04, 12.94, . . .).

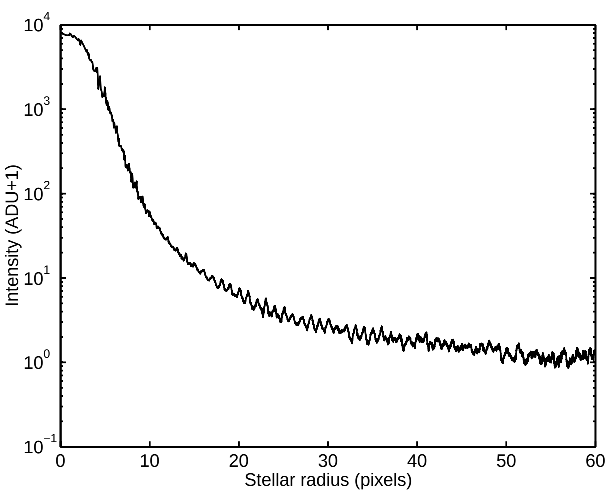

FIG. 5.—Point-spread function for a star with magnitude $m_R = 13.4$. The ADU scale corresponds to an exposure time of 20 minutes.

frames for each chip, using standard routines in IRAF.[19] First, the brighter regions of stellar images were removed from a frame by applying a threshold cut at 1.3 times the modal value. The frames were then modally scaled and combined using the σ clipping procedure of IRAF. This self-consistently removes values that are more than 3 σ from the median. The median of the resultant distribution was used as the flat field. Examination of the distribution of values about the median for any pixel indicated a flat-field accuracy of about 0.85%. This is consistent with the expectation based on Poisson statistics and the typical ADU values ($\sim$300) of the sky frames.

Stellar images on the 20 minute frames generally had FWHM values $\sim 4''$, somewhat in excess of the typical seeing for the system. This resulted from inadequacies of the

[19] IRAF is operated by the Association of Universities for Research in Astronomy, Inc., for the National Optical Astronomical Observatories under cooperative agreement with the National Science Foundation.

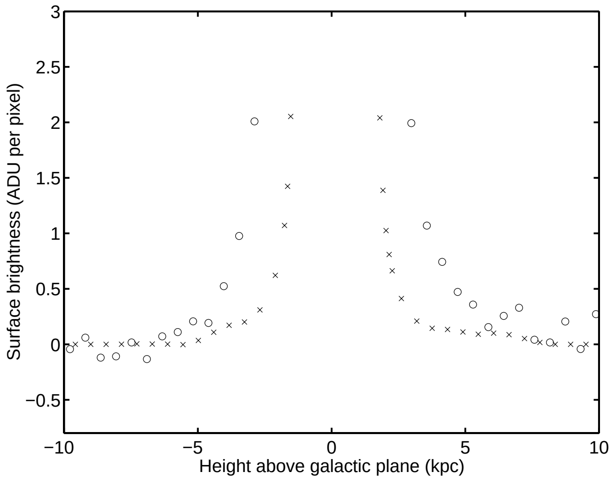

FIG. 6.—Comparison of scattered and observed light in the halo. The circles represent the observed light in the halo, and the crosses, the scattered light from the disk of the galaxy, as described in the text.

tracking system, which is unguided, over the longer-than-normal exposure times employed here. Five of the 20 minute galaxy frames had seeing greater than 4″.4. These were removed from the sample, leaving a total of 16 galaxy frames for further analysis, six with the galaxy on the northeast chip, six on the center chip, and four on the southwest one. These were bias- and cosmic-ray–subtracted, flat-fielded, and stacked into a single frame. Positional alignment was achieved to an accuracy of 1 pixel using six stars. The rotations, translations and scale changes needed for this were carried out using standard IRAF routines. The effective exposure time for the stacked frame is $5\frac{1}{3}$ hr. It is shown in Figure 3. The FWHM seeing is $\approx$4″.0, and the limiting magnitude is $\approx$22.5. Our photometric measurements of IC 5249 were all derived from this 5 1/3 hr frame.

5.2. *Calibration of Photometry*

Following each 20 minute exposure of IC 5249, a 2 minute exposure was made on the same chip. Five uncrowded stars in these exposures with V magnitudes in the range 12–15 and colors $0.8 < B-V < 1.8$ were used to calibrate the photometry. They are shown in Figure 4. Photoelectric measurements of these stars in the B, V, R_C, and I_C passbands were carried out using the 0.6 m Optical Craftsman Telescope at MJUO and standard stars in the Cousins' F region. These measurements were found to satisfy the relationship

$$m_R = m_{\mathrm{instr,red}} + 24.80 \quad (1)$$

to an accuracy of ± 0.05 mag. Here m_R and $m_{\mathrm{instr,red}}$ denote photoelectric and CCD instrumental magnitudes, respectively.[20] We used equation (1) to calibrate the photometry of IC 5249. In terms of surface brightness, it implies that 1 ADU pixel^{-1} corresponds to $\mu_R = 26.35$ mag arcsec^{-2} for a 20 minute exposure.

It is not possible to determine the sky background in the R_C or I_C passbands from the single-passband sky measurements made here ($\sim$300 ADU for 20 minute exposures). Equation (1) implies only that $\mu_R > 20.2$ mag arcsec^{-2}, consistent with the expected value for Mount John (see § 4). Also, we found that the sky level varied during each night, presumably due to the inclusion of airglow lines in the infrared part of the passband that are variable. These variations appear to have been constant over each chip, otherwise the flat-fielding procedure described above would not have yielded results that are consistent with Poisson statistics.

5.3. *Scattered Light*

Scattered light in a telescope, especially at optical surfaces close to the focal plane, may produce an extended halo surrounding a bright object and contaminate results such as those presented below. We estimated the magnitude of this effect using a technique similar to those used by other groups (Morrison et al. 1994; Sackett et al. 1994; Lequeux et al. 1996). The images of some moderately bright, unsaturated, lone stars on stacked galaxy and sky frames were combined by the median value after scaling the intensities. This produced unsaturated images of bright stars that are free of cosmic rays and surrounding stars, from which the point-spread function could be accurately determined. One is shown in Figure 5 for a star with $m_R = 13.4$. Next a truncated version of the $5\frac{1}{3}$ hr galaxy image was formed by excising the portions of the galaxy greater than 1 kpc from the disk, and this was convolved with the point-spread function. A profile of the convolved image at position A is shown in Figure 6. It shows that scattered light, either in the telescope or in the atmosphere, does not cause the extended halo observed around IC 5249.

6. PHOTOMETRY OF IC 5249

6.1. *Photometry of the Disk of IC 5249*

A contour plot of the galaxy derived from the $5\frac{1}{3}$ hr frame is shown in Figure 7. This may be compared with the H I distribution displayed in Figure 1. No flaring or warping is evident in either image. The major- and minor-axis diam-

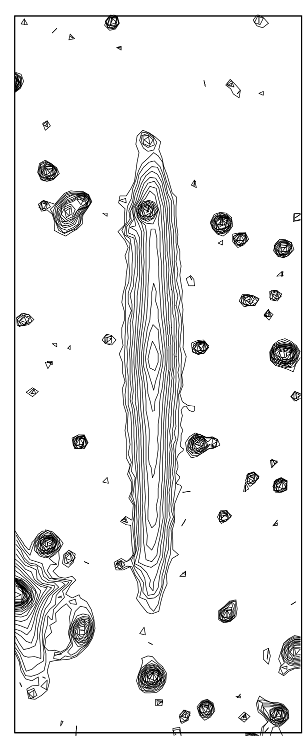

FIG. 7.—Contour plot of IC 5249. The contours are at 21.0, 21.5, 22.0, …, $R_C$mag arcsec^{-2}, and the orientation is the same as in Fig. 3.

[20] The CCD instrumental magnitude was defined in the normal manner, viz., $-2.5 \log$ ADU.

eters of the $R_{23.5}$ isophote are 189″ and 17″, respectively, both very similar to the $I_{23.5}$ values (see § 2).

In what follows, we shall assume $H_0 = 65$ km s^{-1} Mpc^{-1}. This corresponds to a distance of 36 Mpc to IC 5249 and a pixel size on the sky of 0.113 kpc at the galaxy.

In order to characterize the disk and the halo of the galaxy, surface photometry was carried out for the four profiles at the positions labeled A, B, C, and D shown in Figure 8. These profiles are at distances 7.5, 1.1, 5.3, and 11.7 kpc, respectively, from the minor axis of the galaxy, and their widths are 6.4 kpc. The profiles were divided into rectangular bins 1 pixel wide out to a distance of 2 kpc, and thereafter into bins 5 pixels wide. The surface brightness for each bin was determined from the average ADU value. The zero point was taken from the modal value of sky surrounding the galaxy. Light from foreground stars with $m_R < 22.1$ was masked out to a radius where $\mu_R = 28$ mag arcsec^{-2}, as shown in Figure 8. It was found that the results presented below do not depend sensitively on the values of these quantities. It was assumed that foreground stars that are fainter than those that were masked out are uniformly distributed over the image.

The above procedure was found to be adequate in the disk of the galaxy but not in the halo. As other groups have found, large-scale nonuniformities are present in the sky, and these affect the photometry at low light levels (Lequeux et al. 1996; Lequeux et al. 1998). We found that the raw profiles generally decrease monotonically from 0 to about 6 kpc, and thereafter flatten out, but not necessarily to zero. We corrected for this by setting a single baseline for each profile as the best linear fit to the data from −14 to −7 kpc and from +7 to +14 kpc. The fluctuations of the data about the baseline, ±0.15 ADU pixel^{-1}, were used to determine the uncertainty of the procedure. The baseline uncer-

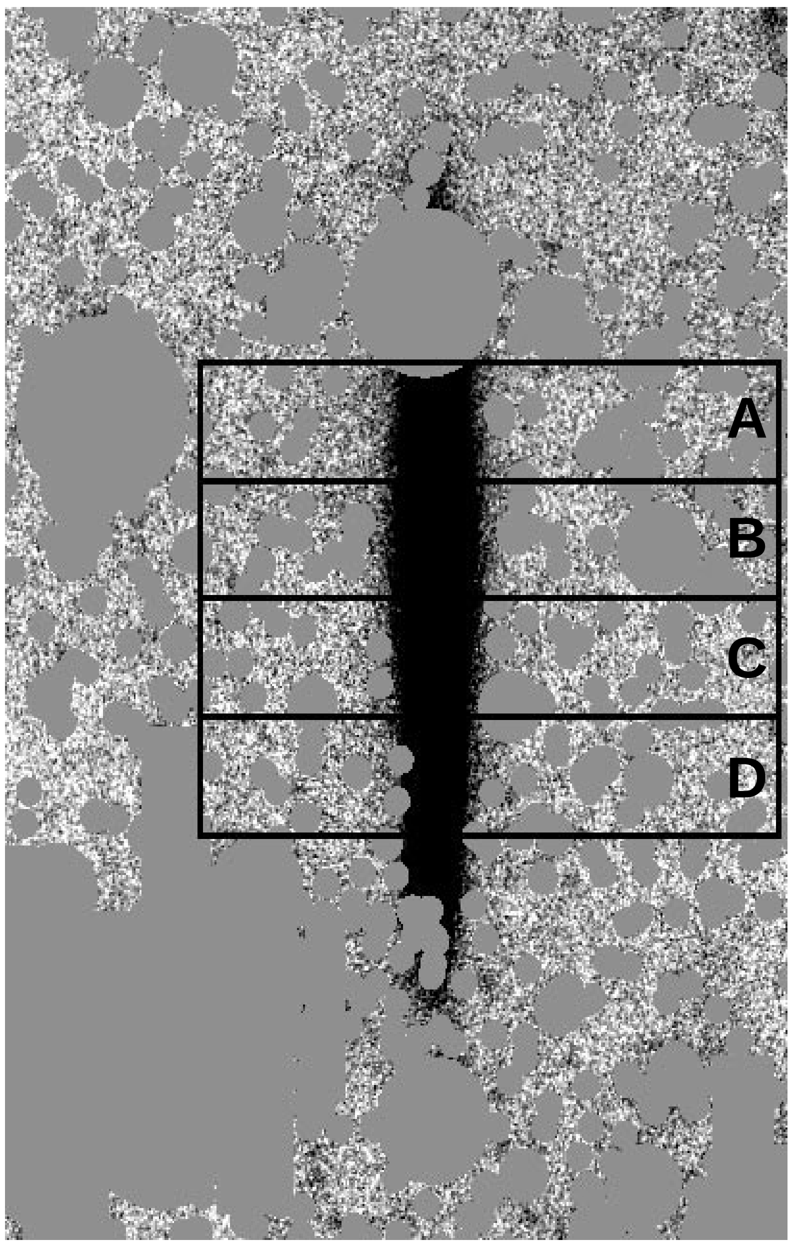

FIG. 8.—Regions A, B, C, and D, where photometry of IC 5249 was carried out, and the region's surrounding foreground stars that were excluded. The gray scale is −1.9 to +3.4.

tainty of ± 0.15 ADU pixel^{-1} was added in quadrature to the statistical uncertainty for each measurement, as shown in Figure 9. A similar procedure was followed by Rudy et al. (1997). Comparison of the baselines in adjacent profiles showed that equivalent results, differing by less than 0.05 ADU pixel^{-1}, would have been obtained if a single baseplane had been used for all four profiles.

The validity of the above procedure was checked by analyzing the data for the three CCD chips separately. The chips are in quite different positions of the focal plane (see § 4), and the large-scale nonuniformities were found to be quite different on them. The largest amounted to $\approx 0.3\%$ of the sky in one region of one chip. However, the corrected profiles for each chip were found to be consistent (Pennycook 1998). Our results suggest the nonuniformities are caused by light from nearby, bright stars being reflected off components of the telescope and the camera. For example, $\sim 1\%$ of the light from two 9th magnitude stars that are near to IC 5249 would have been reflected at the focal plane to the camera window and rereflected to the focal plane. The camera window, which is 2 mm thick and not antireflection-coated, is spaced 30 mm from the focal plane. These stars would have each produced large-scale nonuniformities of ~ 27 mag arcsec^{-2} or $\sim 0.2\%$ of the sky.

Transverse and longitudinal surface profiles for the stacked galaxy frame are shown in Figures 10 and 11. For $r > 18$ kpc, the longitudinal profile appears to decline much more rapidly than predicted by the exponential model. It is not possible to determine from the present data if there is a sharp cutoff to the galaxy in the longitudinal direction, or if it disappears smoothly into the sky. Comparison with the longitudinal I-band profile of Mathewson et al. (1992) indicates that the color index $R - I \approx 0.4$ mag arcsec^{-2} along the major axis.

For the purpose of systematically analyzing the surface profiles, the following model of the three-dimensional luminosity density of the galaxy was used,

$$L(R, z) = L_0 e^{-R/H} e^{-|z|/h} . \quad (2)$$

Here R and z denote cylindrical radial and transverse coordinates relative to the disk, respectively, and H and h radial and transverse scale height parameters, respectively. L_0 is the central luminosity density of the galaxy. The exponential in the transverse direction is an approximation to a locally isothermal three-dimensional sheet (Kruit & Searle 1981).

The surface profiles were fitted to line integrals of the luminosity density assuming the galaxy to be perfectly edge-

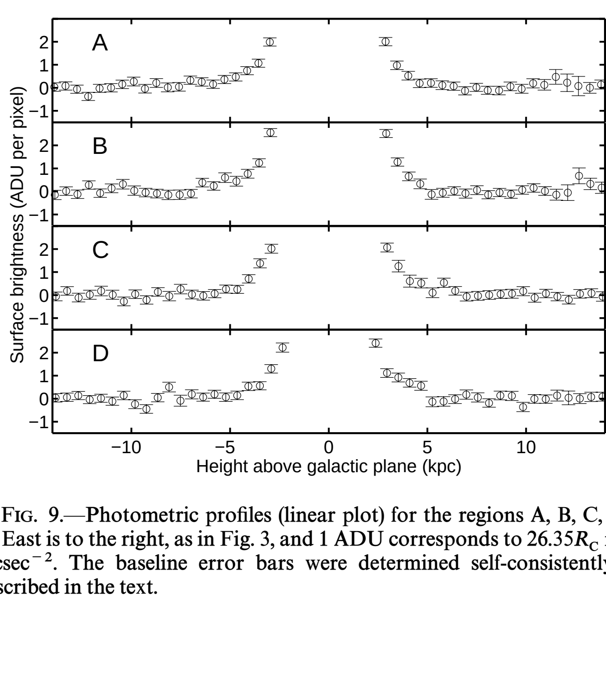

FIG. 9.—Photometric profiles (linear plot) for the regions A, B, C, and D. East is to the right, as in Fig. 3, and 1 ADU corresponds to $26.35 R_C$ mag arcsec^{-2}. The baseline error bars were determined self-consistently as described in the text.

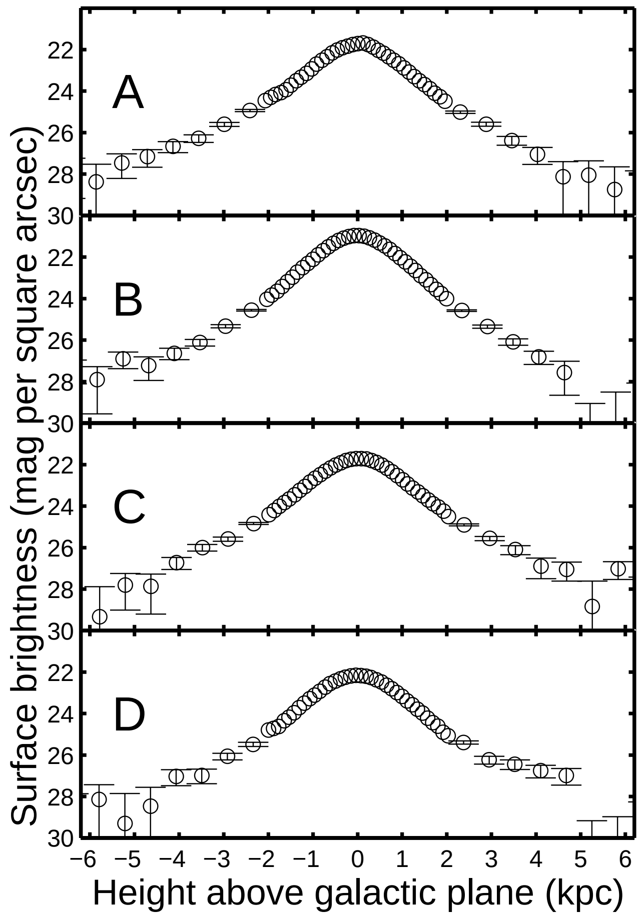

FIG. 10.—Photometric profiles (log plot) for the regions A, B, C, and D of IC 5249 in the R_C passband. The error bars include baseline and statistical errors added in quadrature.

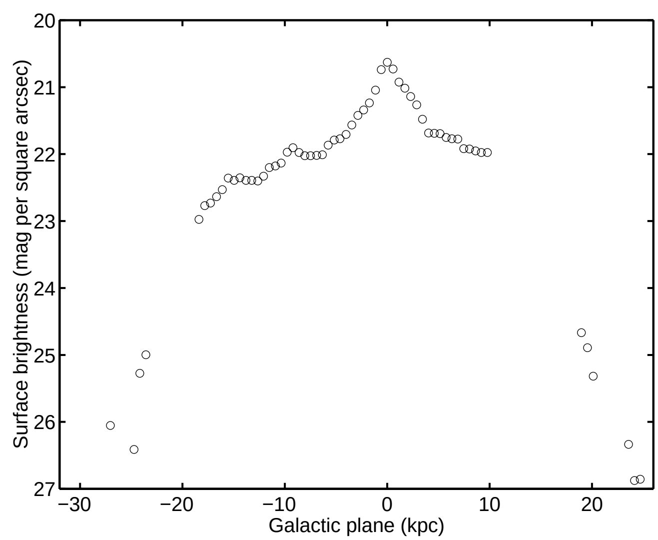

FIG. 11.—Longitudinal profile of IC 5249 in the R_C passband. The photometry was performed with 5 × 5 pixel bins. Gaps in the profile occur where bright foreground stars are present.

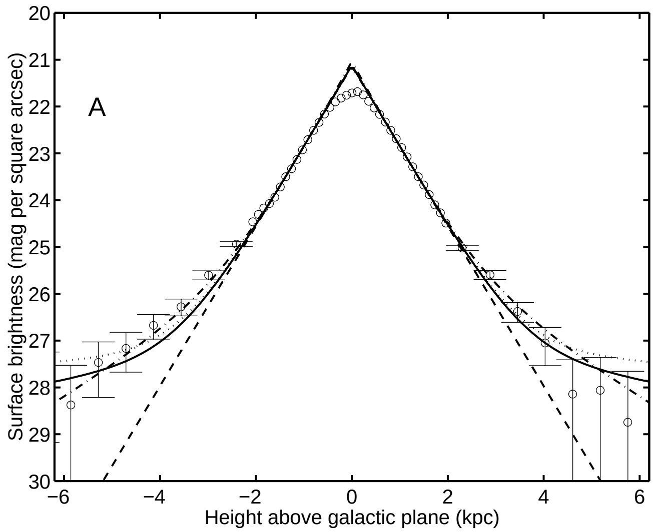

FIG. 12.—Model fits to profile A. The dashed lines are the best single exponential fit (eq. [2]) from 1–2 kpc with $h = 640$ pc and H $\approx$ 11 kpc. The dashed-dotted curve is the best fit for the "thick-disk" model with the parameters given in Table 1, the dotted curve is the best fit for the "dark matter" model with the parameters given in Table 2, and the solid curve is the best fit for the "globular cluster" model with the parameters given in Table 3.

on. For a profile at distance d from the minor axis, the surface luminosity was assumed to take the form

$$\int_{-\infty}^{\infty} L_0 e^{-R/H} e^{-|z|/h} dl = 2L_0 e^{-|z|/h} \int_0^{\infty} e^{-R/H} dl$$
$$= 2L_0 e^{-|z|/h} \int_0^{\infty} e^{-\sqrt{(d^2+l^2)}/H} dl , \quad (3)$$

and the final integral was performed numerically. Good fits (see Figs. 12–14 below) to the data for $|z| = 0.5$–2.0 kpc for profiles A, C, and D were obtained with the above model with the following values of the scale heights: $h \approx 640 \pm 10$ pc and $H \sim 11 \pm 2$ kpc. The former value corresponds to an estimated transverse scale height of $h \approx 600 \pm 40$ pc when the effect on the observations of the seeing is included.

The scale heights for IC 5249 are larger than for most disk galaxies, implying IC 5249 is an optically extended

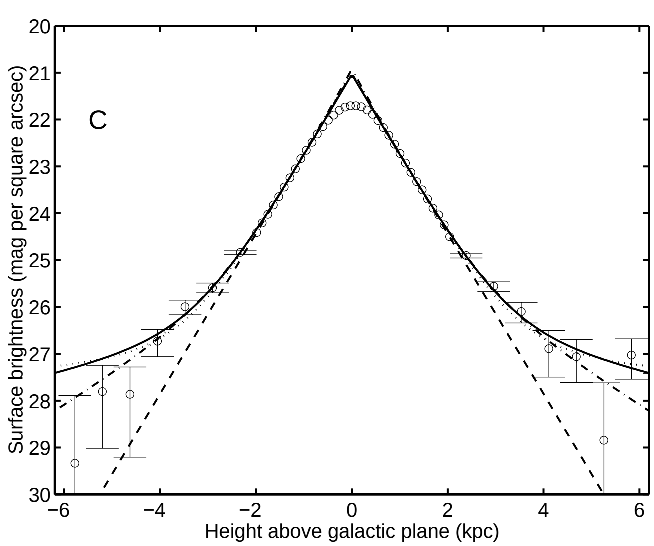

FIG. 13.—Model fits to profile C as in Fig. 12

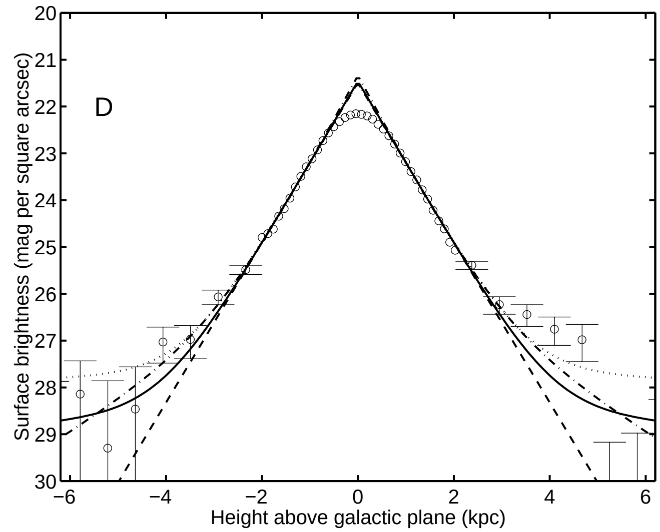

FIG. 14.—Model fits to profile D as in Fig. 12

galaxy in both the radial and transverse directions. The corresponding values for NGC 5907 are 467 pc and 5.1 kpc, respectively (Morrison et al. 1994). The central R_C surface brightness of IC 5249 within $\sim$1 kpc of the major axis and $\sim$4 kpc of the minor axis is $\sim$1 mag arcsec^{-2} dimmer than that of NGC 5907, signifying that IC 5249 is a relatively low surface brightness galaxy. The integrated luminosity derived from equation (2) is $m_{R_C} = 13.6 \pm 0.2$. This corresponds to an absolute R_C magnitude of 19.2 ± 0.2. This may be compared with the R-band value expected on the basis of the luminosity–line width relation of Tully (1997), viz., 19.5 ± 0.5.

Equation (2) predicts a central surface luminosity of $2L_0 H$ when a galaxy is viewed edge-on and $2L_0 h$ when viewed face-on. These values neglect the effect of dust. Our best fit to profiles A, C, and D corresponds to values of $\sim 20.8 R_C$ mag arcsec^{-2} and $\sim 24.3 R_C$ mag arcsec^{-2} for these quantities for IC 5249. The former value slightly underestimates the actual central edge-on surface brightness, which is (see Fig. 11) $20.6 \pm 0.1 R_C$ mag arcsec^{-2}. The discrepancy is presumably caused by dust and the presence of a small nuclear bulge in IC 5249. The likely presence of a nuclear bulge was the reason for excluding profile B, which intersects the bulge, in the determination of the scale heights of the galaxy. The face-on central brightness predicted above is only an approximation to what the true value would be, because it does not include the effects of dust, nonexponential structure, and a viewing angle not precisely equal to 90°. We shall address these details in a forthcoming paper on observations of IC 5249 at other wavelengths.

TABLE 1

PARAMETERS FOR THE "THICK-DISK" MODEL

Parameter	Value
h_1 (pc)	570
H_1 (kpc)	11 ± 2
h_2 (pc)	1690
H_2 (kpc)	6 ± 1
$L_{0,2}/L_{0,1}$	0.135
Reduced χ^2	1.2

TABLE 2

Parameters for the "Dark Matter" Model

Parameter	Corresponding Value
h (pc)............	630
H (kpc)	11 ± 2
$L_{\rm dm}/L_0$	4.5×10^{-6}
Reduced χ^2......	1.7

6.2. *Photometry of the Halo of IC 5249*

Photometry of the halo of IC 5249 was the prime goal of the present study. It is clear from Figure 10 that the luminosity of the halo generally exceeds that predicted by the exponential model as defined by equation (2). The data were therefore tested against various models that include extra sources of light in the halo. Three specific models were tested, a "thick-disk" model, a "dark matter" model, and a "globular cluster" model. The thick-disk model was defined by a luminosity function

$$L(R, z) = L_{0,1}\, e^{-R/H_1} e^{-|z|/h_1} + L_{0,2}\, e^{-R/H_2} e^{-|z|/h_2} , \quad (4)$$

where $L_{0,1}$, H_1, and h_1 parametrize the thin disk of the galaxy, and $L_{0,2}$, H_2, and h_2 the thick disk. The dark matter model was defined by the equation

$$L(r, R, z) = L_0\, e^{-R/H} e^{-|z|/h} + L_{\rm dm}(r/H)^{-2} , \quad (5)$$

where r denotes Galactocentric radius, and L_{dm} is a parameter characterizing the luminosity density of a visible halo that is presumed to be distributed like dark matter. The globular cluster model was defined as

$$L(r, R, z) = L_0\, e^{-R/H} e^{-|z|/h} + L_{\rm gc}(r/H)^{-3.5} , \quad (6)$$

where $L_{\rm gc}$ characterizes the model, and the associated power (-3.5) was chosen to mimic the known distribution of globular clusters in the Galaxy. The above definitions were used in regions exterior to the central bulge only.

TABLE 3

Parameters for the "Globular Cluster" Model

Parameter	Corresponding Value
h (pc)............	620
H (kpc)	11 ± 2
$L_{\rm gc}/L_0$...........	2.8×10^{-4}
Reduced χ^2......	1.7

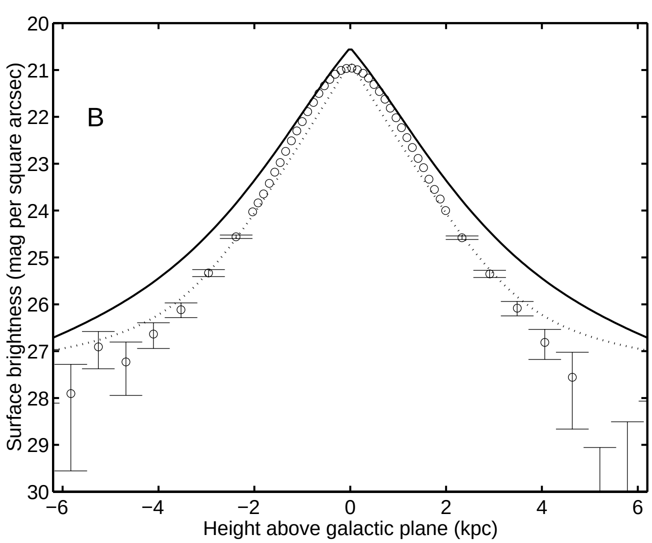

FIG. 15.—Best fits to profiles A, C, and D applied to profile B. This profile intersects the Galactic bulge.

The profiles A, C, and D were used to determine best-fit parameters for the above models, and profile B was subsequently used as a test. Best fits to the A, C, and D profiles were obtained with the values of the parameters given in Tables 1, 2, and 3. These fits are shown in Figures 12–14. Figure 15 shows a comparison of the data for profile B, which intersects the Galactic bulge. It is clear that the globular cluster model is ruled out by the data at large distances from the disk. This appears to be true regardless of the possible presence of a nuclear bulge in IC 5249. The present data for IC 5249 are not quantitatively accurate enough to distinguish between the thick-disk and dark matter models. However, the thick-disk model requires quite different radial scale heights for the thin and thick disks. This would seem to indicate that thick and thin disks in a galaxy can evolve independently or that IC 5249 does not possess a thick disk.

7. TOTAL MASS OF VISIBLE STARS IN THE HALO OF IC 5249

In the absence of color information on the halo, the identity of the stars being detected cannot be determined from the above photometry. However, an upper limit on their total mass can be deduced, and this can be used to constrain their identity as follows.

Suppose stars of one type only are present in the halo and that these are distributed with spatial density $\propto r^{-2}$, consistent with dark matter model defined by equation (4). Denote the mass, luminosity and absolute magnitude of the halo stars by m_h, L_h, and M_h, respectively. Then it may easily be shown that their total mass $M_{\rm C}$ inside a cutoff radius $r_{\rm C}$ is

$$M_{\rm C} = 4\pi m_h r_{\rm C} L_{\rm dm} H^2/L_h , \quad (7)$$

and that their surface brightness at "impact parameter" b from the center of the galaxy is

$$\int_{-\infty}^{\infty} L_{\rm dm}(H/r)^2\, dl = L_{\rm dm} H^2 \pi/b . \quad (8)$$

Equation (8) is, of course, valid irrespective of the inclination angle of the disk of the galaxy to the line of sight. It implies a surface brightness in mag arcsec^{-2}

$$\mu = M_h - 2.5 \log\,(\pi L_{\rm dm} H^2 k^2/bL_h) . \quad (9)$$

Here $k = 10\pi/3(60)^3$ pc. Equations (7) and (9) imply

$$\mu = M_h - 2.5 \log\,(M_{\rm C}/m_h) - 2.5 \log\,(k^2/4br_{\rm C}) . \quad (10)$$

Equation (10) may be used to estimate the total mass of visible stars in the halo, as follows: The best fit to the present data, as shown in Figures 12–14, has $\mu = 27.61 \pm 0.5\ R_{\rm C}$ mag arcsec^{-2} at $b = H = 11$ kpc. This implies that

$$\log\,(M_{\rm C}/m_h) \approx M_h/2.5 - 11.04 - \log\,[k^2/(44 r_{\rm C}\ {\rm kpc})] . \quad (11)$$

TABLE 4

GALACTIC MASS FRACTION OF MAIN-SEQUENCE HALO STARS IN IC 5249

m_h ($M_\odot$)	M_h	$M_c/M_\odot$	Limit on Mass Fraction (percent)
0.13……	11.37	1.90×10^{10}	66.6
0.15……	10.88	1.40×10^{10}	49.0
0.20……	10.05	8.7×10^{9}	30.4
0.30……	9.07	5.2×10^{9}	18.4
0.40……	8.35	3.6×10^{9}	12.6
0.50……	7.40	1.9×10^{9}	6.6
0.60……	6.24	7.8×10^{8}	2.7
0.70……	5.24	3.6×10^{8}	1.3
0.80……	3.93	1.2×10^{8}	0.4

NOTE.—M_h and m_h denote the absolute R_C magnitude and mass of the halo stars, and M_c the total mass of these stars ($\pm 50\%$) inside Galactocentric radius 24.5 kpc if the mass and spatial distributions of the halo stars are Dirac and r^{-2} functions, respectively. The rightmost column gives the 95% confidence upper limit on the Galactic mass fraction of these stars inside 24.5 kpc.

Here M_h denotes the absolute magnitude of the halo stars in the R_C passband. The uncertainty in the photometry in the halo corresponds to an uncertainty in M_C/m_h of $\sim 50\%$.

Baraffe et al. (1998) calculated absolute magnitudes of metal-poor low-mass stars. Using their values for halo stars with [M/H] ~ -1.3 to -1.5, we obtain the values given in Table 4 for the total mass of low-mass stars in the halo that are distributed like dark matter inside a Galactocentric radius of 24.5 kpc. The total masses given there correspond to delta-function mass distributions and are therefore conservative upper limits only. Furthermore, if the spatial distribution of main-sequence stars in the halo is actually less extended than the dark matter distribution defined by equation (5), then the upper limits in Table 4 could be further reduced. This would be the case if, for example, the thick-disk model, defined by equation (4), is a better approximation than the dark matter model.

We conclude from Table 4 that a halo comprised entirely of main-sequence stars heavier than 0.13 $M_\odot$ is excluded, and that less than 20% of the halo can be made up of main-sequence stars heavier than 0.30 $M_\odot$. The results are shown graphically in Figure 16 and compared with corresponding Galactic results that were obtained by gravitational microlensing by the EROS and MACHO collaborations (Alcock et al. 1998; Afonso et al. 1999) and by Gilmore & Unavane (1998) by infrared photometry of external galaxies.

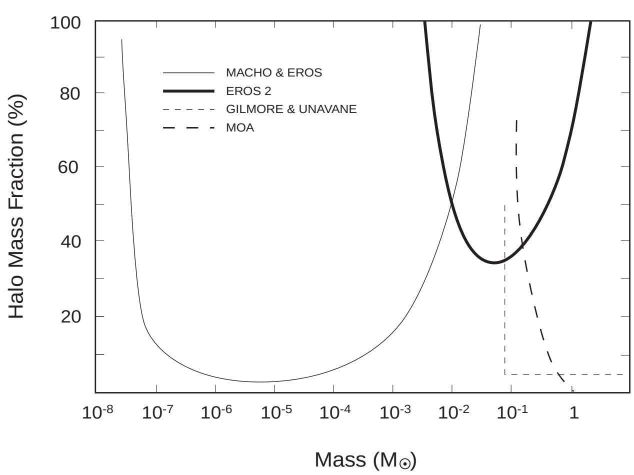

FIG. 16.—Upper limit to the contribution of main-sequence halo stars to the total mass of IC 5249 inside a Galactocentric radius of 24.5 kpc (*thick-dashed line*). Corresponding results for other galaxies obtained by gravitational microlensing and infrared photometry are also included. The thin solid line denotes the upper limit for low-mass objects of any type in the halo of the Milky Way reported by Alcock et al. (1998) using the gravitational microlensing technique, and the thick solid line is a similar limit due to Afonso et al. (1999). The thinned dashed line denotes an upper limit for main-sequence stars that was obtained by Gilmore & Unavane (1998) for four external galaxies by infrared photometry.

8. CONCLUSIONS

The edge-on Sc/Sd galaxy IC 5249 has a relatively extended disk characterized by a scale height and scale length of 600 $\pm$ 40 pc and 11 $\pm$ 2 kpc, respectively. Its rotation curve rises linearly out to a radius of 7 kpc and then appears to flatten out at $\sim$100 km s^{-1}. Additional light to that predicted by an exponential disk is present at distances greater than 3 kpc from the disk. The distribution of light out to 5 kpc from the disk may be fitted, within the existing experimental uncertainty, by either a thick disk or by a halo distributed like dark matter. In either case, main-sequence stars heavier than 0.30 $M_\odot$ can account for 20% of the halo of IC 5249 at most, and a halo made up entirely of main-sequence stars heavier than 0.13 $M_\odot$ is excluded. Further measurements are required to determine the rotation curve of IC 5249 to larger radii and the precise abundance of low-mass main-sequence stars in its halo.

The authors thank J. Lequeux, H. Morrison, and P. Sackett for discussions, the Department of Physics and Astronomy of the University of Canterbury for the provision of telescope time, the Marsden and Science Lottery Funds of NZ, the Ministry of Education, Science, Sports and Culture of Japan, the KEK Laboratory of Japan, and the Research Committee of the University of Auckland for financial support.

REFERENCES

Abe, F., et al. 1997, in Proc. 12th IAP Conf., Variable Stars and the Astrophysical Returns of Microlensing Surveys, ed. R. Ferlet, J.-P. Maillard, & B. Raban (Gif-sur-Yvette: Ed. Frontieres), 75
Afonso, C., et al. 1999, A&A, 344, 63
Alcock, C., et al. 1997, ApJ, 491, 436
———. 1998, ApJ, 499, L9
Baraffe, I., Chabrier, G., Allard, F., & Hauschildt, P. 1997, A&A, 327, 1054
Briggs, F. H. 1990, ApJ, 352,15
da Costa, L. N., Pellegrini, P. S., Davis, M., Meiksin, A., Sargent, W. L. W., & Tonry, J. L. 1991, ApJS, 75, 935
Flynn, C. 1999, in ASP Conf. Ser. 666, The Galactic Halo, ed. B. K. Gibson, T. S. Axelrod, & M. E. Putman (San Francisco: ASP), 387
Fuchs, B. 1995, A&A, 303, L13
Gilmore, G., & Unavane, M. 1998, MNRAS, 301, 813
Lequeux, J., Dantel-Fort, M., & Fort, B. 1996, A&A, 296, L13
Lequeux, J., Combes, F., Dantel-Fort, M., Cuillandre, J. C., Fort, B., & Mellier, Y. 1998, A&A, 334, L9
Levasseur, P., Carignan, C., & Byun, Y.-I. 1992, Proposal No. C212 to the Australia Telescope National Facility
Mathewson, D. S., Ford, V. L., & Buchhorn, M. 1992, ApJS, 81, 413
Morrison, H. L., Boroson, T. A., & Harding, P. 1994, AJ, 108, 1191
Pennycook, G. S. 1998, MS thesis, Univ. Auckland
Roberts, M. S., & Haynes, M. P. 1994, ARA&A, 32, 115

Rudy, R. J., Woodward, C. E., Hodge, T., Fairfield, S. W., & Harker, D. E. 1997, Nature, 387, 159
Sackett, P. D., Morrison, H. L., Harding, P., & Boroson, T. A. 1994, Nature, 370, 441
Stubbs, C. 1999, in ASP Conf. Ser. 666, The Galactic Halo, ed. B. K. Gibson, T. S. Axelrod, & M. E. Putman (San Francisco: ASP), 503
Tinney, C. G. 1999, Nature, 397, 37
Tully, R. B. 1997, in Cosmological Parameters and the Evolution of the Universe, ed. K. Sato (IAU Symposium 183, Kyoto, August 1997)
van der Kruit, P. C., & Searle, L. 1981, A&A, 95, 105
Wright, A. E., Griffith, M. R., Burke, B. F., & Ekers, R. D. 1994, ApJS, 91, 111